Wannier-Stark States in Finite Superlattices

M. Kast,* C. Pacher, G. Strasser, and E. Gornik
Institut für Festkörperelektronik, Technische Universität Wien, Floragasse 7, A 1040 Wien, Austria

W. S. M. Werner
Institut für Allgemeine Physik, Technische Universität Wien, Wiedner Hauptstrasse 8-10, A 1040 Wien, Austria
(Received 1 March 2002; published 5 September 2002)

Individual Wannier-Stark states are resolved in a current experiment over a wide electric-field range for a 5 and 4 period finite superlattice utilizing a hot-electron transistor. The observed field dependence of the tunneling transmission through the various states directly resembles the progressive localization of the wave functions. The basic transport through Wannier-Stark states in short-period superlattices is identified to be coherent. By tuning the Wannier-Stark state splitting with electric field into the optical phonon energy, the opening of new LO-phonon mediated transport paths is observed.

DOI: 10.1103/PhysRevLett.89.136803 PACS numbers: 73.21.Cd, 72.80.Ey, 73.23.Ad, 73.40.Gk

The idea of growing multilayers of alternating semiconductor alloys with different band offsets made it possible to realize artificial crystals, so-called superlattices. The large number of design parameters as, for example, the material system, the layer thickness, the doping concentration, etc. makes it possible to engineer the band structure of such crystals [1]. In an unperturbed superlattice, the strong coupling of the electronic eigenstates of adjacent wells leads to the formation of minibands which are separated by minigaps. In superlattices with a finite number N of periods, each single miniband is formed by N eigenstates which are delocalized over the whole superlattice length. Applying an external electric-field perpendicular to the layer planes alters the quantum mechanical confinement between the neighboring wells and leads to a splitting and a localization of the states which are then given by the Wannier-Stark states [2]. Until the suggestion of Esaki and Tsu in the year 1970 [3], to realize superlattices by using semiconductor heterostructures, the Wannier-Stark effect could not be verified in conventional crystals with common measurement techniques. The first studies of biased semiconductor superlattices were performed on n-i-n structures, where the quantification of the Wannier-Stark splitting was mainly done by using optical techniques as electroabsorption [4], photoluminescence [5], photocurrent [5], and electroreflectance [6] measurements.

In transport experiments, there are two main problems to determine the Wannier-Stark splitting in a semiconductor superlattice: One is the presence of an inhomogeneous electric-field unavoidable in two-terminal superlattice structures; the second is the electric-field induced localization of the Wannier-Stark states. The localization length inside the superlattice is inversely proportional to the applied electric field which leads to a quenching of the coherent hot-electron transport through the individual Wannier-Stark states. In two-terminal device transport studies, the existence of the Wannier-Stark effect could be verified only by measuring negative differential velocity of hot electrons in biased superlattices [7]. England *et al.* [8] and Aggarwal *et al.* [9] reported tunneling measurements of electronic states in superlattices in which the transition from a miniband to a sequential coupled well structure is reported. Current resonances appear for specific alignments of neighboring Wannier-Stark states. A clear quantification of the Wannier-Stark splitting and the Wannier-Stark localization from direct current measurement has never been reported thus far to our knowledge. The understanding of electron transport in biased superlattice structures is of fundamental interest for the development of novel semiconductor devices such as quantum cascade lasers and Bloch oscillators.

In this work, we use the concept of a hot-electron transistor [10–15] to study hot-electron transport in undoped biased superlattices. The conduction band structure of the device is shown in the inset of Fig. 1(a). An energy tunable electron beam is generated at the tunneling barrier and reaches the superlattice after traversing a highly doped n-GaAs base layer and a slightly n-doped drift region. The amount of purely ballistic electrons transmitted through the superlattice and measured as the collector current I_C is at the order of a few percent. The vast majority of the electrons have lost energy by optical phonon emission in the drift region and are collected in the base contact since the injection energy is always well above the LO-phonon energy. The static transfer ratio ($\alpha = I_C/I_E$) directly represents the probability of an injected electron to be transmitted through the superlattice. Beltram *et al.* [16] reported scattering induced tunneling of hot electrons through biased superlattices using a three terminal device with a fixed injection energy of the hot-electron beam. The resonances appeared only for special alignments of the Wannier-Stark states with the electron injection energy. The special property of the three terminal device used in this work allows a tuning of the energy

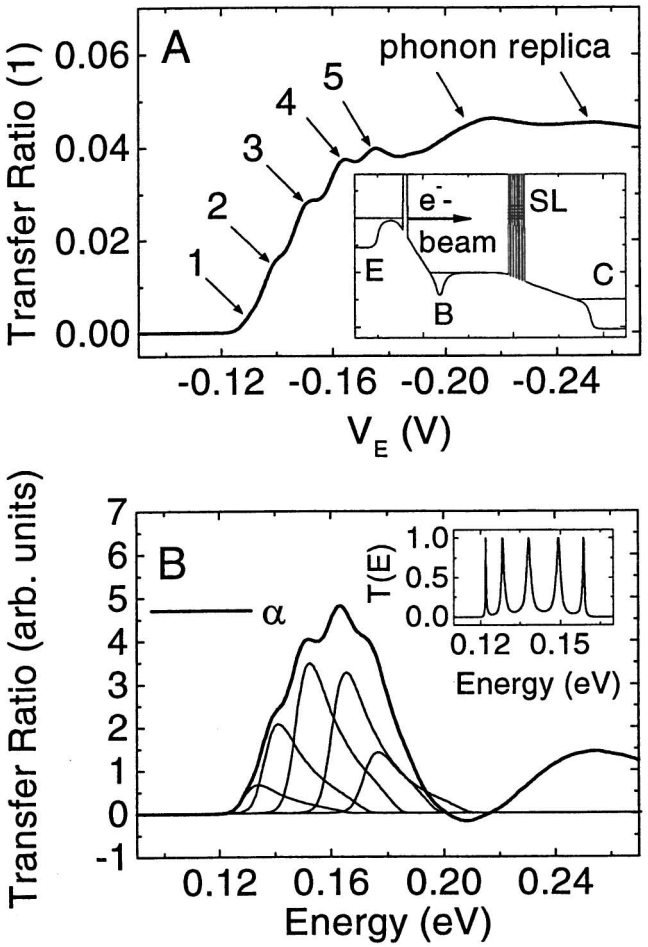

FIG. 1. (a) Measured transfer ratio $\alpha = I_C/I_E$ of a 5 period SL (solid line) vs emitter bias ($\approx$ electron injection energy). Features which indicate tunneling of ballistic electrons through the corresponding resonant states are marked 1–5. (Inset) Conduction band diagram of a three terminal device along the growth direction with an external electric field applied at the collector. (b) Background-removed transfer ratio compared to the convolution of the ballistic electron energy distribution (obtained in Ref. [15]) with the calculated transmission resonances shown in the inset. (Inset) Calculated transmission function $T(E)$ of the 5 period superlattice: 3.3 nm AlGaAs barriers and 3 nm GaAs wells.

of the injected electron distribution independent of the electric field applied to the superlattice. Consequently, it is possible to apply a homogeneous electric field to the superlattice. The other problem—to study localized Stark states which do not allow transport through the superlattices—can be overcome by the use of a scattering mechanism which can induce transitions between weakly overlapping Wannier-Stark states. In this experiment, LO-phonon scattering provides such an incoherent transmission channel inside the superlattices.

Three terminal devices were designed with different undoped superlattice structures between base and collector. The first superlattice consists of 5 periods of 3.5 nm $Al_{0.3}Ga_{0.7}As$ barriers and 3 nm GaAs wells; the second superlattice consists of 4 periods of 4 nm $Al_{0.3}Ga_{0.7}As$ barriers and 3.2 nm GaAs wells. For these superlattice parameters, the lowest miniband is positioned between 122 and 158 meV for the 5 period SL and between 120 and 143 meV for the 4 period SL. The three terminal devices are grown by molecular beam epitaxy and fabricated by standard photolithographic and wet etching techniques. The emitter and collector currents were measured as a function of negative emitter bias at 4.2 K in a common base configuration using a parameter analyzer. Figure 1(a) shows the transfer ratio of the 5 period superlattice as a function of the electron injection energy. For energies below the first state, no collector current is observed, since the ballistic electrons are reflected at the superlattice. The onset at $V_E = -130$ mV indicates the beginning of electron tunneling through the first miniband. At energies above the first miniband, the ballistic electrons are reflected at the superlattice. However, there is an additional contribution to the measured transfer ratio which is due to longitudinal optical (LO) phonon emission ($\hbar\omega_{LO} = 36$ meV) in the GaAs drift region [15]. This inelastic background in the transfer ratio is removed by a deconvolution procedure [17]. Figure 1(b) shows the comparison of the background-removed transfer ratio with the convolution of the ballistic electron distribution [15] with the calculated transmission resonances [shown in the inset of Fig. 1(b)]. The peak amplitudes resemble the different linewidths of the transmission resonances.

Hot electron transport in biased superlattices is investigated as a function of the collector bias up to $V_C = 400$ mV. In Fig. 2, the second derivatives of the transfer ratios are plotted as a function of the collector bias. The peaks which indicate electron transport through the corresponding Wannier-Stark states are marked from 1 to 5 for the 5 period SL (1 to 4 for the 4 period SL). The potential applied to the superlattice pulls the miniband to lower energies and causes a down shift of the peaks. The increase of the energy spacings between the individual peaks as a function of the electric field gives direct evidence of the Wannier-Stark character of the states. At high injection energies, peaks $4'$ and $5'$ ($3'$ and $4'$) are indicating transport due to phonon replicas occurring in the drift region. The energetic positions of the 5 (4) individual peaks in the transfer ratio at $V_C = 0$ V fit best to calculated [18] subband energies using superlattice parameters of 3.3 nm AlGaAs barriers and 2.9 nm GaAs wells for the 5 period superlattice and 3.7 nm AlGaAs barriers and 3 nm GaAs wells for the 4 period superlattice. The deviation to the nominal superlattice parameters lies within one monolayer for GaAs and AlGaAs.

The Wannier-Stark splitting is determined from the transfer ratios shown in Fig. 2. The experimental Wannier-Stark splitting is measured as a function of the collector bias, whereas the theoretical Wannier-Stark splitting is calculated as a function of the electric field applied to the superlattice [18]. By comparing the Wannier-Stark splitting at the highest collector bias ($V_C = 400$ mV) with the calculated Wannier-Stark

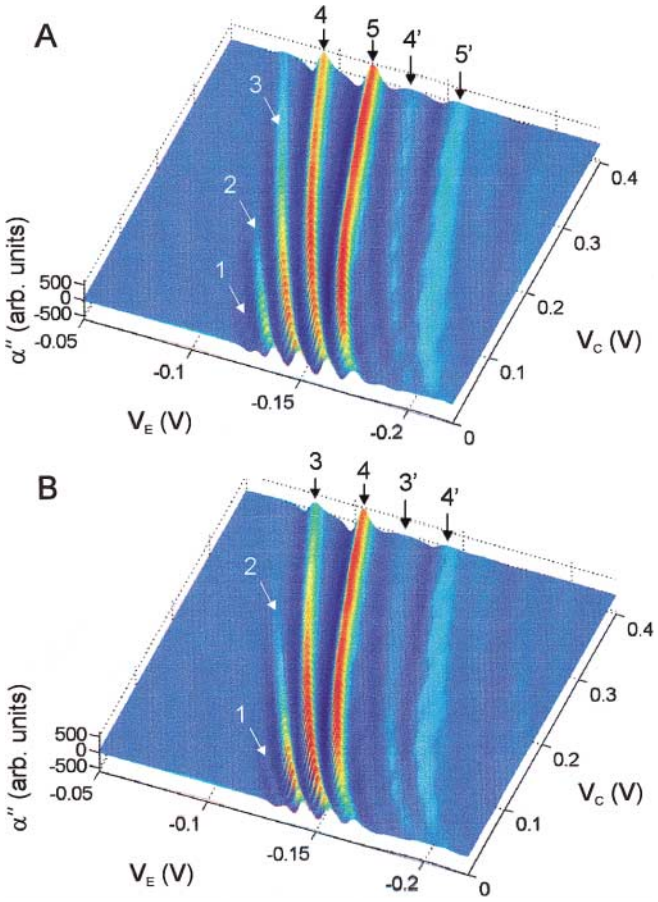

FIG. 2 (color). (a) Second derivatives of the transfer ratio vs emitter bias at different collector biases for the 5 period superlattice. (b) Second derivatives of the transfer ratios vs emitter bias at different collector biases for the 4 period superlattice.

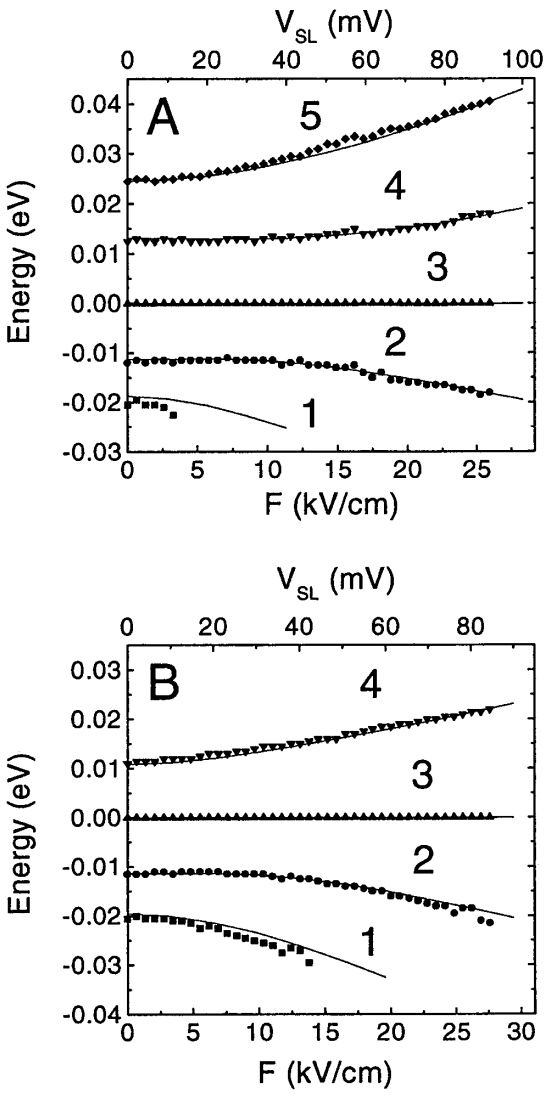

FIG. 3. (a) Measured Wannier-Stark states (symbols) vs superlattice bias V_{SL} of the 5 period superlattice compared to the calculated Wannier-Stark splitting (solid lines) vs electric field F. (b) Wannier-Stark states (symbols) of the 4 period superlattice compared to calculations (solid lines).

splitting, a corresponding electric-field value is obtained which directly gives the relation between the collector bias scale and the electric-field scale. Figure 3 shows the measured peak positions (symbols) relative to the position of peak 3 for both superlattices as a function of the electric field. The experimental results are in excellent agreement to the theoretical Wannier-Stark splitting (solid lines) [18] up to electric fields of $F = 25.9$ kV/cm for the 5 period superlattice and $F = 27.6$ kV/cm for the 4 period superlattice, respectively.

Besides the Stark splitting, it is especially interesting to analyze the electric-field induced localization of the Wannier-Stark states. In transport experiments, the amplitudes of the current resonances directly resemble the quantum mechanical transmission of the individual states as seen in Fig. 2. A comparison of the electric-field dependence of the normalized peak amplitudes in the transfer ratios with the expected Wannier-Stark localization amplitudes for the 4 period superlattice is shown in Fig. 4, which directly provides information about the transport mechanisms through each single state. For states 1 and 2, an excellent agreement between measured and calculated transmission is found. For peaks 3 and 4, the experimental findings exceed the coherent predictions: While peak 3 first shows a transmission according to the coherent path, an additional contribution to the current starts at 10 kV/cm and becomes larger than the coherent part, passes through a maximum until it decreases at fields above 20 kV/cm. Peak 4 increases above the coherent part already at zero bias and increases in two steps.

We have previously ruled out interface roughness scattering for a 5 period superlattice [14] as scattering always induces a current component proportional to the electric field which is not observed. Electron-electron scattering can be ruled out due to an extremely low carrier concentration in the device. The only incoherent transmission channel is LO-phonon scattering which occurs only for transition energies E_{ij} exceeding $\hbar\omega_{LO}$. For the first and second Wannier-Stark state (WSS1, WSS2), LO-phonon

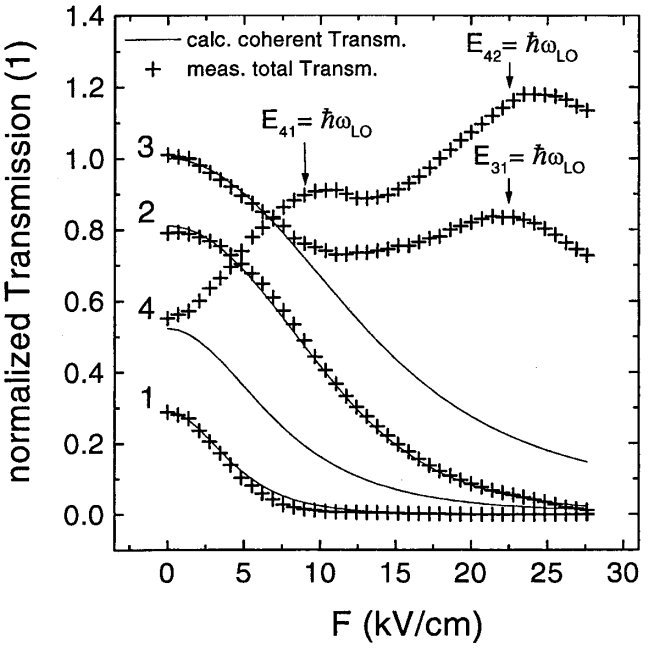

FIG. 4. Measured normalized transmission per states as a function of the electric-field (crosses) compared to the calculated normalized coherent transmissions of the individual Wannier-Stark states for the 4 period superlattice (solid lines). The arrows mark critical fields where the inter-Wannier-Stark state splittings are equal to the optical phonon energy.

scattering can be neglected because the transition energy is much smaller than $\hbar\omega_{LO}$ over the whole bias range. As a consequence, transport through these states is purely coherent.

For WSS3 and WSS4, additional current is observed at electric fields, where transition energies E_{31}, E_{41}, and E_{42} exceed $\hbar\omega_{LO}$ at $F_{31} = 21$ kV/cm, $F_{41} = 9$ kV/cm, and $F_{42} = 22$ kV/cm. However, an increase of the incoherent transport is already observed well below F_{31}, F_{41}, and F_{42} (marked with arrows in Fig. 4). This can be understood by taking into account that the ballistic electron distribution has a finite width in the plane perpendicular to the current direction (normal dispersion) of $\Delta E = 7$ meV [15]. This leads to the situation that those electrons have a total energy larger than the transition energy between different WSSs. They are able to emit LO phonons at transition energies of $E_{ij} = \hbar\omega_{LO} - \Delta E$. For WSS4, this condition is fulfilled for transition 4-1 at flat band conditions and for transition 4-2 at $F = 17.6$ kV/cm. The increase in the peak amplitude resembles, thus, the tuning of the Stark ladder with increasing electric field until the peak of the distribution is resonant with the Stark state splitting of $\hbar\omega_{LO}$.

The results clearly show that incoherent transmission channels induced by optical phonons add additional current. For WSS3 only one channel is possible which is resonant at 21 kV/cm. The increase in current is significant and the channel transmission is comparable to the coherent path at zero bias. For WSS4, the first phonon channel (4-1) becomes possible at $F_{41} = 9$ kV/cm, giving about the same current as for WSS3; when the condition for phonon channel 4-2 is reached, the second channel adds about the same amount of current to the transmission. The data thus clearly show individual channels of incoherent transport.

In conclusion, we present a study of electron transport through undoped biased superlattices. The individual Wannier-Stark states in the first miniband of a 5 (4) period superlattice are resolved up to electric fields of $F = 25.9$ kV/cm ($F = 27.6$ kV/cm) in a direct current experiment. From the measured transfer ratios, the exact superlattice parameters are determined. The basic transport through Wannier-Stark states is identified to be coherent. The transport mechanism through higher lying localized states is found to result from an interplay between coherent and incoherent transport as a function of the applied electric field. LO-phonon induced individual channels are found to contribute to the transmitted current. This way, we have a method at hand which enables a systematic study of transition rates for different scattering processes in semiconductor heterostructures.

This work was partly supported by the Society for Microelectronics (GMe, Austria) and the Austrian Science Fund (FWF) Grants No. SFB F016 and No. Z24.

*Email address: michael.kast@tuwien.ac.at

[1] F. Capasso, Science **235**, 172 (1987).
[2] G. H. Wannier, Phys. Rev. **117**, 432 (1960).
[3] L. Esaki and R. Tsu, IBM J. Res. Dev. **14**, 61 (1970).
[4] J. Bleuse, G. Bastard, and P. Voisin, Phys. Rev. Lett. **60**, 220 (1988).
[5] E. E. Mendez, F. Agulló-Rueda, and J. M. Hong, Phys. Rev. Lett. **60**, 2426 (1988).
[6] P. Voisin and J. Bleuse, Phys. Rev. Lett. **61**, 1639 (1988).
[7] A Sibille, J. F. Palmer, F. Mollot, and H. Wang, Phys. Rev. Lett. **64**, 52 (1990).
[8] P. England, M. Helm, J. R. Hayes, J. P. Harbison, E. Colas, and L. T. Florez, Appl. Phys. Lett. **54**, 647 (1989).
[9] R. J. Aggarwal *et al.*, Appl. Phys. Lett. **57**, 707 (1990).
[10] M. Heiblum, M. I. Nathan, D. C. Thomas, and C. M. Knoedler, Phys. Rev. Lett. **55**, 2200 (1985).
[11] J. R. Hayes, A. F. J. Levi, and W. Wiegmann, Phys. Rev. Lett. **54**, 1570 (1985).
[12] M. V. Petrov and S. A. Lyon, Appl. Phys. Lett. **70**, 3263 (1997).
[13] C. Rauch, G. Strasser, K. Unterrainer, B. Brill, and E. Gornik, Appl. Phys. Lett. **70**, 649 (1997).
[14] C. Rauch, G. Strasser, K. Unterrainer, W. Boxleitner, and E. Gornik, Phys. Rev. Lett. **81**, 3495 (1998).
[15] M. Kast, C. Pacher, G. Strasser, and E. Gornik, Appl. Phys. Lett. **78**, 3639 (2001).
[16] F. Beltram *et al.*, Phys. Rev. Lett. **64**, 3167 (1990).
[17] W. S. M. Werner, Phys. Rev. B **52**, 2964 (1995).
[18] G. Bastard, Phys. Rev. B **24**, 5693 (1981); we calculate the energetic positions of the Wannier-Stark states using a simple transfer matrix method including nonparabolicity.